Proceedings of the 1991 IEEE
International Conference on Robotics and Automation
Sacramento, California - April 1991

DESIGN OF A FOUR DEGREE-OF-FREEDOM FORCE-REFLECTING MANIPULANDUM WITH A SPECIFIED FORCE/TORQUE WORKSPACE

Paul A. Millman
J. Edward Colgate

Department of Mechanical Engineering
Northwestern University

Abstract

Performance of force-reflecting hand controllers, also called manual interfaces or manipulanda, is at present limited more by mechanical design than by computing hardware. Some of the important mechanical features of a high performance manual interface are: low inertia, low friction, high stiffness, backdriveability, high output force capability, multiple degrees-of-freedom, and sizeable range of motion. A four degree-of-freedom manipulandum, which utilizes a three degree-of-freedom parallel-link mechanism, was designed to incorporate the above features. The kinematic design of the manipulator motivated the definition of a force/torque workspace as the volume of operation within which certain maximum desired endpoint forces and torques can be achieved, given actuators of limited output. The design requires low actuator torques, is small in size, and does not approach joint limits in the workspace.

1 Introduction

Force-reflecting manual interfaces, also called manipulanda or hand controllers, enable human operators to send and receive information through the modalities of motion and force. As such, the devices can provide useful links to telemanipulators and other mechanical systems, and to computers (e.g. virtual realities).

Hand controllers have been used in teleoperation to supplement visual feedback to the human operator. In bilateral or force-reflecting telemanipulation, loads measured or evaluated at the endpoint of the remote manipulator are fed back to the operator as forces on the hand. The purpose of the device described in this paper is primarily, although not not exclusively, to serve as a control input to a micro-manipulator. Such a system could be used to perform micro-surgery, micro-assembly, or biological experimentation. [2, 6, 9]. Hunter and colleagues have built a micro-manipulator for the last purpose, specifically the study of individual living muscle cells [9]. A force-reflecting manual interface to their micro-manipulator lets an operator manipulate and "feel" the cells.

This leads to another important application of hand controllers, as means to manipulate and explore unfamiliar environments, such as micro-environments, and to literally "get a feel" of the physics unique to those environments. An exciting demonstration of this concept is the "magic wrist", a six degree-of-freedom (d.o.f.) device with which an operator interactively controls a scanning-tunneling microscope and "feels" surfaces at the atomic level [8]. Hand controllers can also be used for manipulation and exploration in computer generated, or virtual, environments. Chemists at The University of North Carolina have used a six d.o.f. serial manipulator to dock computer generated images of molecules onto larger organic molecules under the influence of simulated molecular forces [12]. Using hand controllers, researchers can also investigate the mechanical properties and control systems of human limbs. Adelstein studied severe arm tremor in patients with Parkinson's disease using a two d.o.f. force-reflecting joystick [1].

Unfortunately, the usefulness of hand controllers has often been limited by poor performance related to their mechanical design. The purpose of the research reported here was to develop a hand controller with the high performance needed for basic research in micro-teleoperation, human manipulation, and human limb mechanics.

2 Design Goals

The principle objective of a force-reflecting manual interface is to impart forces and torques to the operator's hand as he or she moves the endpoint. It is essentially a "force/torque display", and should be able to generate a wide range of dynamic behaviors, i.e. admittances. The following is a list of important features for a high performance manipulandum.

- **Low inertia**: Inertia lowers the admittance of the manipulandum. A device capable of high endpoint admittance provides the operator with more sensitivity at low force levels, which is especially important when working in low impedance environments. Although some of the inertia felt by the operator can be masked by feedback control, not all can be [1].
- **Low friction**: Friction also lowers endpoint admittance, thereby degrading force resolution and increasing force thresholds (force required to cause motion at handle).
- **High stiffness**: Low stiffness in the links, joints, or transmission, or low servo stiffness can degrade feel when trying to simulate "hard" (low admittance) environments, e.g. walls. Low stiffness (or large manipulator inertia) also results in a low natural frequency for the manipulator, which can cause closed

loop instability when force sensors and actuators are noncollocated.

- **Backdriveability**: Feedback control is only marginally successful in making a nonbackdrivable manipulator appear backdriveable [3]. Low transmission ratios are needed for the manipulator to be mechanically backdriveable.
- **Zero or near-zero backlash**: Backlash in the drive train results in sudden changes in endpoint force and can cause closed loop instability. Backlash can be eliminated by using direct drive or by careful design of the drive train.
- **Gravitational counterbalancing**: To avoid operator fatigue, the force of gravity should be statically counterbalanced. Counterweights (which add to the mass of the manipulator) and springs are two means of counterbalancing.
- **Sizeable volume of operation**: A small workspace may limit the operator's ability to manipulate, while one that is too large may cause operator fatigue.
- **Multiple degrees-of-freedom**: Six degrees of freedom is ideal for a general purpose hand controller, but multiple degrees-of-freedom are at odds with other design goals.
- **Output force capabilities matched to human operator**: A person can generate large static forces and torques with his or her arm which must be matched by the manipulandum to simulate stiff or "hard" environments.

In their review and evaluation of hand controller designs, Fischer, Daniel and Siva provide an excellent discussion of the above issues [5].

Other designers have cited some of the same design goals, which are reflected in their designs. Notably, Adelstein's two d.o.f. manipulandum is direct drive with both motors mounted at the base. It can successfully simulate a variety of dynamic behaviors, ranging from a lightweight mass, to a spring-loaded detent, to a rigid wall [1]. Russo extended Adelstein's design to add a third d.o.f. [14]. Craver and Tesar designed a parallel-link, three d.o.f. shoulder module to be stiff, lightweight and "strong" [4]. The parallel architecture has the advantage of, again, locating all the motors at the base. The four d.o.f. design presented in this paper incorporates a three d.o.f. parallel-link manipulator similar to the shoulder module. The remainder of this paper describes the design of the four d.o.f. hand controller (which is currently being built), focusing on the selection of kinematic parameters for the parallel-link mechanism.

3 Description of Hand Controller

The hand controller will have three planar degrees-of-freedom (x,y,θ), and translation normal to the xy plane (i.e. z). This number of degrees-of-freedom is a compromise between functionality, complexity and cost. Four degrees-of-freedom are sufficient to enable dextrous manipulation (such as planar assembly) and are compatible with the observation of a micro-telemanipulator under a microscope. When working under a microscope, the limited depth of field constrains an operator to a nearly planar workspace.

Figure 1 is a schematic of the design. The three planar degrees-of-freedom are provided by the parallel mechanism shown in Figure 2. Three motors for this mechanism drive the links l_1, which are connected to the rigid triangle by links l_2. The motor shafts are connected to the driven links, l_1, through prismatic joints (zero-backlash, low friction ball splines) which are actuated in common by a fourth motor to provide the fourth d.o.f. In other words, the entire three d.o.f. mechanism slides up and down as a unit on three spline shafts.

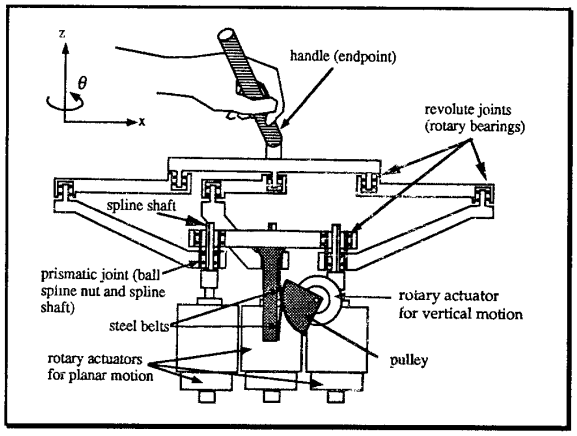

Figure 1. Schematic of four degree-of-freedom (x,y,z,θ) hand controller.

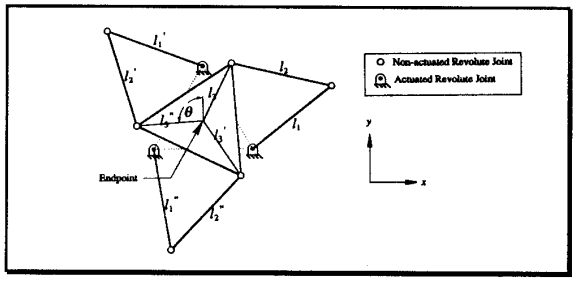

Figure 2. Kinematic diagram of parallel-link mechanism providing three planar degrees of freedom (x,y,θ).

An important feature of the design is that all four motors are base-mounted, making the links low inertia. Also, the parallel structure is very rigid compared to serial designs. Direct drive is employed to eliminate transmission problems such as compliance, friction, and non-backdriveability. A disadvantage of the parallel mechanism is its complicated kinematic transformations, but computational hardware advances, including DSP's and parallel architectures,make the computational burden bearable. Redundant position sensors at the joints also simplify the computations.

4 Kinematic Design of Planar Mechanism

4.1 Reduction of Number of Design Parameters

Vertical motion of the hand controller is decoupled with motion of the planar mechanism, and the kinematics of the fourth d.o.f. are trivial. Selecting appropriate values of the kinematic parameters for the parallel-link mechanism, however, provides a challenge.

Making the mechanism symmetric reduces the number of design parameters. No reasons exist for wanting a non-symmetric workspace, or non-symmetric actuators, so the three branches of the mechanism are the same (i.e. $l_1=l_1'=l_1''$, $l_2=l_2'=l_2''$, and $l_3=l_3'=l_3''$). For the same reason, the three motors are located 120 degrees apart, on the perimeter of a circle of radius, R. In addition, the driven and connecting links are equal lengths ($l_1=l_2$). This simplifies the design and prevents the "elbow joint" between each pair of driven and connecting links from reaching its joint limits over a large range of motion. The importance of avoiding joint limits (configurations where adjacent links are parallel) is explained more fully in Sections 4.3 and 4.5. The resulting design parameters are:

- Length of the driven and connecting links: $l_1=l_2$
- Length of the inner links: l_3
- Radius of circle on which actuators lie: R.

4.2 The Force/Torque Workspace

Quantitative criteria are needed to evaluate different designs. As stated earlier, the manipulandum must exhibit some range of motion, or volume of operation, and the ability to generate forces and torques at the endpoint throughout the range of motion. Actuators must also be chosen to provide the necessary input torques, the magnitudes of which depend on *i*) the kinematic design, *ii*) the desired endpoint forces and torques, and *iii*) the desired range of motion. The design of the mechanism was therefore further simplified by specifying, *a priori*, the volume of operation, and the minimum acceptable upper limit on achievable endpoint force and torque.

The best design can be described as the smallest manipulator with the smallest actuators that can generate certain desired endpoint loads everywhere in the specified workspace. A small mechanism is desirable to minimize link compliance and inertia, and small actuators are desirable to minimize cost and rotor inertia.

The mechanism is designed for x and y translation within a circle of 8 inch diameter, and for vertical translation of 3.5 inches (unlike translation in the horizontal plane, vertical translation is limited by link interference, not by choice). The choice of a *circular* workarea is prompted by the symmetry of the planar mechanism about three axes, as well as convenience. The mechanism is designed to provide 90° of rotation at the endpoint, with the additional qualification that the range be the same 90° (relative to a fixed coordinate system) throughout the translational workspace.

This volume of operation is appropriate for tasks that involve principally finger and wrist motions. In experiments with a variety of joints, Mesplay and Childress found that people performed position control, pursuit-tracking tasks better using finger and wrist joints as control inputs than they did using the elbow joint [11]. Langolf, Chaffin and Foulke report similar results with subjects performing Fitt's repetitive movement tasks at different amplitudes [10]. Although the subjects in these studies performed only simple tasks, without force feedback, the results suggest that for a variety of tasks, humans are more dextrous using their fingers and wrist than using gross arm movement.

The manipulandum is also designed to ensure that anywhere within the four dimensional workspace, 10 lbs of force (in all directions) and 12 in-lbs of torque (in both directions) can be generated at the endpoint. These levels of force and torque were judged to be sufficient, after performing simple experiments with human subjects grasping a 6-axis force sensor.

The *force/torque workspace* is defined as the volume of operation in taskspace (four dimensional in this case) in which a prescribed set of endpoint forces and torques can be achieved given actuators of known limited output. For this design, the desired four dimensional volume of operation described above is constrained to be inside the force/torque workspace with prescribed endpoint loads of 10 lbs and 12 in-lbs, and with actuator torque limits to be calculated. The concept of the force/torque workspace is very appropriate in the design of hand controllers, where range of endpoint forces and torques is as important as range of motion. It should be useful in the design of other types of manipulators as well.

The design procedure for the three d.o.f. mechanism consists of calculating the required acuator torque for a set of kinematic parameters ($l_1=l_2$, l_3 and R), given the constraint stated earlier, that the desired volume of operation be a subset of the force/torque workspace of the manipulator. Additional constraints are that the links not interfere with one another in any configuration, and that the joints not approach their limits. These two points will be clarified in Sections 4.3 and 4.5. The final design is chosen based on the length of the links and the magnitude of the actuator torques.

4.3 Singularities

Singularities, configurations of the manipulator at which, instantaneously, the actuators cannot control motion and force at the endpoint, are clearly unacceptable within the volume of operation. Two kinds of singularities are depicted in Figure 3. The most obvious singularities occur when an "elbow" joint (joint between driven and connecting links, l_1 and l_2) reaches a joint limit (the angle between links is either zero or 180°). When this occurs, the axial force and velocity of the connecting link cannot be controlled by the motor, and a degree of freedom is lost (Figure 3(a)) [7, 13]. A second type of singularity is described by the condition that lines passing through the connecting links intersect at a point (including the case of intersection at infinity) [7,, 13].

In the configuration shown in Figure 3(b), the motors are unable to resist a rotation of the endpoint about the point of intersection. The existence of these singularities suggests that, in the center of the workspace, adjacent links should be nearly perpendicular to each other.

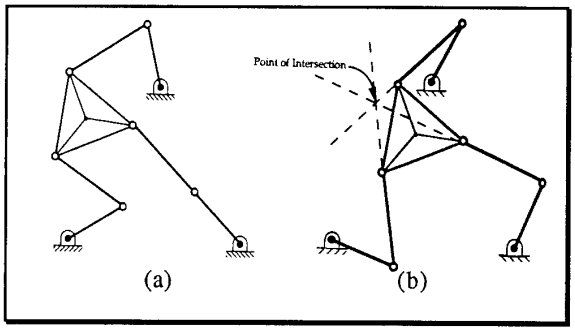

Figure 3. Singular configurations of mechanism in which a joint limit is reached (a), and lines through the connecting links intersect at a point (b).

4.4 Mappings between Endpoint and Actuator Coordinates

In order to evaluate the actuator torques needed at points within the volume of operation, a mapping is needed from task-space "forces" (endpoint force and torque) to actuator-space torques. Nonlinear kinematic equations map endpoint position coordinates of the planar mechanism (x,y,θ) to actuator position coordinates (ϕ_1,ϕ_2,ϕ_3) [7, 13]. From these equations the 3×3 Jacobian matrix for the mechanism can be evaluated [7, 13]. The Jacobian linearly maps endpoint velocities to actuator velocities. This mapping can be written as

$$J\dot{x}_e = \dot{\phi}_a \quad , \tag{1}$$

where J is the configuration dependant Jacobian, $\dot{x}_e$ is the vector of endpoint velocities, and $\dot{\phi}_a$ is the vector of actuator velocities.

The mapping from endpoint forces to actuator torques, involving the inverse transpose of the Jacobian, can be written as

$$\tau_a = [J^T]^{-1} F_e \quad , \tag{2}$$

where τ_a is the three vector of actuator torques, and F_e is the three vector of endpoint forces. Defining T as the inverse transpose of the Jacobian, and substituting into Equation (2), we have

$$\tau_a = TF_e \quad , \tag{3a}$$

which, in expanded form, is

$$\begin{bmatrix} \tau_a^1 \\ \tau_a^2 \\ \tau_a^3 \end{bmatrix} = \begin{bmatrix} T_{11} & T_{12} & T_{13} \\ T_{21} & T_{22} & T_{23} \\ T_{31} & T_{32} & T_{33} \end{bmatrix} \begin{bmatrix} F_e^x \\ F_e^y \\ \tau_e \end{bmatrix} . \tag{3b}$$

Once the Jacobian is calculated at a particular position and orientation of the endpoint, the motor torques are calculated as:

$$\tau_d^i = T_{i1} F_e^x + T_{i2} F_e^y + T_{i3} \tau_e \quad , \; i=1,2,3 \; . \tag{4}$$

4.5 Kinematic Parameter Selection

The available motor torques can be represented as a cube in actuator-torque coordinates (see Figure 4(a)). Each face is defined by the continuous stall torque of a DC motor. Continuous stall torques of the motors are chosen to define the actuator torque limits because this ensures that the motors will not overheat and that they can provide larger dynamic torques if needed. In Figure 4(b), the desired endpoint loads are represented as a cylinder in endpoint force space whose boundaries are defined by the maximum desired endpoint loads (i.e. 10 lbs and 12 in-lbs).

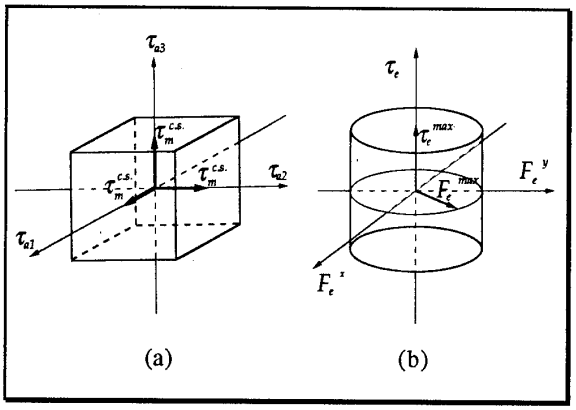

Figure 4. (a) Continuous stall torques of actuators represented in actuator torque space. (b) Maximum desired endpoint loads represented in endpoint force/torque space.

It is true then, that at every position (x,y,θ) in the force/torque workspace, the cylindrical "volume" of endpoint loads maps inside the cubic "volume" of continuous stall torques. It is mathematically simple to test if an endpoint position is in the force/torque workspace using the transformation from endpoint loads to actuator torque space.

From Equation (4) we find that, for a particular position and orientation of the endpoint, the "volume" of endpoint loads maps inside the "volume" of continuous stall torques if

$$\sqrt{(T_{i1})^2 + (T_{i2})^2} \; |F_e^{max}| + |T_{i3}\tau_e^{max}| \le |\tau_a^i|_{c.s.} \quad , \; i=1,2,3 \tag{5}$$

where F_e^{max} is the maximum endpoint force (10 lbs), τ_e^{max} is the maximum endpoint torque, and $|\tau_a^i|_{c.s.}$ is the actuator continuous stall torque for motor i. This inequality represents the worst case of Equation (4), when F_e and τ_e are at their greatest magnitude and the

vector $F_e^x \hat{i} + F_e^y \hat{j}$ is aligned with the vector $T_{i1}\hat{i} + T_{i2}\hat{j}$. If, for a particular design, the inequality is satisfied for all three motors at all points in the prescribed volume of operation, then the design has the required force/torque workspace.

In a specific configuration, τ_r, the actuator torque required for the endpoint position to lie within the force/torque workspace, can be calculated by modifying Equation (6). The modified equation is

$$max\left(\sqrt{(T_{i1})^2 + (T_{i2})^2}\ \left|F_e^{max}\right| + \left|T_{i3}\tau_e^{max}\right|\right) = \tau_r\,, \quad i=1,2,3 \tag{6}$$

where the notation is intended to mean that a worst case actuator torque is calculated for each of the three motors, and the greatest of the three is τ_r , The motor continuous-stall torque required for a particular design is the maximum value of τ_r in the volume of operation. A program was written in the C programming language to automate the process of calculating the continuous stall torques for a large number of designs. For each design, the program scanned the planar workarea and the full 360° of rotation to find the 90° range of motion (relative to a fixed reference frame) where the necessary continuous stall motor torque is minimized .

Approximately 500 combinations of the three design parameters were evaluated over the following ranges.

- Radius of circle on which motors lie:R=3.6-8.4 in.
- Lengths of driven and connecting links:l_1=l_2=3.6-10 in.
- Length of inner links:l_3 =1.0 - 6.0 in.

The lower limit on R comes from the limit on how closely the motors can be spaced. Most designs were unacceptable because either certain positions in the desired volume of operation cannot be reached, or the required actuator torque is prohibitively great. As stated previously, the best designs minimize the kinematic parameters and the required motor torque. Note that minimizing R minimizes the mass and compliance of the structure that actuates the three spline nuts in common for out of plane motion. Three of the best designs are listed in TABLE I.

TABLE I
THREE DESIGNS OF THE PLANAR MECHANISM

R (in.)	l_1=l_2 (in.)	l_3 (in.)	τ_r (in-lbs)	θ range (deg.)
3.6	6.6	5.4	79	110-200
3.6	6.6	4.2	102	125-215
3.6	6.6	3.6	108	125-215

The first design listed requires a motor torque of 79 in-lbs, which is the lowest torque of any design evaluated. The other two designs require greater motor torques but have shorter length parameters. Figure 5 is a series of mesh plots of required motor torque (τ_r) for the second design listed in TABLE I. The maximum torque is quite uniform throughout the workspace.

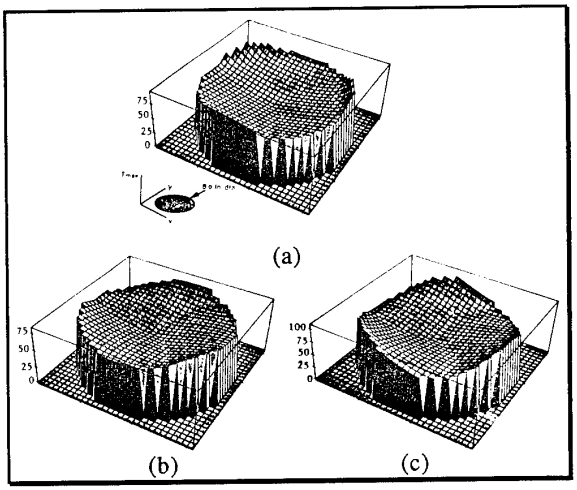

Figure 5. Mesh plots of the maximum actuator torques (in-lbs) needed to produce a minimum of 10 lbs endpoint force in any direction and 12 in-lbs endpoint torque using the second design from TABLE I. The required actuator torque is evaluated at points inside the 8 in. workarea and at endpoint orientations of (a) 125°, (b) 170°, and (c) 215°.

Other considerations in the design include avoiding the overlap of links that result in link interference, and the avoidance of elbow joint limits. Elbow joint angles in the neighborhood of the joint limits (180° and 0°) are avoided because of the associated dynamics (increased inertia in certain directions) of the links near those singular points, not because of degrading static endpoint forces and torques. In fact, near these singularities (but not at them) static force generation capabilities are very good.

To investigate these issues, Vogle graphics libraries in C were used on a Sun workstation to animate kinematic models of a few designs. The first of the three designs above, with the longest inner links, exhibits positions in which the elbow joints nearly "straighten out". The second and third designs, with smaller inner links, exhibit this problem to a lesser extent.

All three designs in TABLE I have configurations for which one link overlaps another. Stairstepping the links, i.e. connecting the links so that the inner, connecting and driven links are each at different levels, prevents interference between links of different type. The type of interference problem that arises when, say, the distal end of a driven link overlaps the proximal end of another driven link, can be solved by angling the driven links upward from the motors (see Figure 1). The connecting links are similarly angled upward from the elbow joints . Note that the driven links have to be angled in any case, to avoid them striking the spline shafts of the other two motors. This interference, between spline shafts and driven links, limits vertical motion to 3.5 inches. The final design, depicted in Figure 6, is a further refinement of the length parameters.

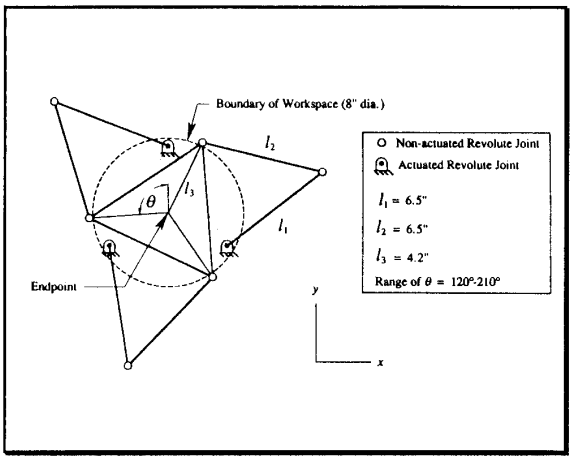

Figure 6. Planar mechanism design.

5 Detailed Design

The detailed design of the hand controller is complete, and work is progressing on construction. A number of features in the detailed design will help make this device stiff and light. The actuators for planar and vertical motion are Electo-Craft brushless DC motors S-4075 and S-3007, respectively. Brushless motors have the advantages of low friction, low rotor inertia, and small size.

Bearing housings at the joints will be machined from aluminum. The links will be filament wound graphite tubes, which are approximately half the density and 1.5 times the stiffness of aluminum. In order to avoid the added mass of a counterweight, a constant force spring will counterbalance the force of gravity on the mechanism.

Lumped parameter models of the structural dynamics of the manipulator predict that its lowest natural frequency will be approximately 100 Hz.

6 Conclusion

A four d.o.f. manipulandum was designed incorporating a three d.o.f. parallel-link mechanism, which has the advantages of being rigid and allowing base-mounted actuators. The force/torque workspace was defined as the volume of operation in taskspace in which a prescribed set of endpoint forces and torques can be generated, given actuators of limited output. Selecting values for the kinematic parameters involved numerically evaluating approximately 500 designs. For each design, the actuator torques required to generate the desired endpoint loads within the specified volume of operation were calculated. The final design was chosen to minimize mechanism and actuator size.

Acknowledgement

The authors gratefully acknowledge the support of the Engineering Foundation, Grant RI-A-90-4.

References

[1] B. D. Adelstein. *A virtual environment system for the study of human arm tremor*. PhD thesis, Department of Mechanical Engineering, M.I.T., June, 1989.

[2] S. Charles, R. E. Williams, and T. L. Poteat, In *Symposium on Robotics*,369-374. ASME Winter Annual Meeting, Chicago, Illinois, 1988.

[3] J. E. Colgate. "On the inherent limitations of force feedback compliance controllers," *Robotics Research*, K. Youcef-Toumi, and H. Kazerooni, editors. ASME, New York, December, 1989.

[4] W. M. Craver, D. Tesar. "Force and deflection determination for a parallel 3 dof robotic shoulder module," *Proceedings of the ASME Design Technical Conferences- 21st Biennial Mechanisms Conference*, Chicago, IL,1990, pp. 473-79.

[5] P. Fischer, R. Daniel, and K. V. Siva. "Specification and design of input devices for teleoperation," *Proceedings of the IEEE International Conference on Robotics and Automation*, Cincinnatti, OH, 1990, pp. 540-545.

[6] T. Fukuda, K. Tanie, and T. Mitsuoka. "A new method of master-slave type of teleoperation for a micro-manipulator system," In *Proceedings of the IEEE Micro Robots and Teleoperators Workshop*, Hyannis, MA, 1987.

[7] C. Gosselin, J. Angeles. "The optimum Kinematic design of a planar three-degree-of-freedom parallel manipulator," *Journal of Mechanisms, Transmissions, and Automation in Design*, vol. 110, March, 1988 pp. 35-41.

[8] R. L. Hollis, S. Salcudean, D. W. Abraham. "Toward a tele-nanorobotic manipulation system with atomic scale force feedback and motion resolution," *Proceedings of the IEEE MicroElectro Mechanical Systems Conference*,

[9] I. W. Hunter, S. Lafontaine, P. M. F. Nielsen, P. J. Hunter, and J. M. Hollerbach. "Manipulantion and dynamic mechanical testing of microscopic objects using a tele-micro-robot system," *Proceedings of the IEEE Micro Electro Mechanical Systems Conference*, Salt Lake City, Utah, 1989, pp.102-106,

[10] G. D. Langolf, D.B. Chaffin, and J. A. Foulke. "An investigation of Fitt's law using a wide range of movement amplitudes," *Journal of Motor Behavior*, vol. 8, no. 2, pp. 113-128, 1976.

[11] K. P. Mesplay and D. S. Childress. "Capacity of the human operator to move joints as control inputs to prostheses,". *Modeling and Control Issues in Biomechanical Systems*, vol. 12, pp. 17-25, 1988.

[12] O. Ming, D.V. Beard, F. P. Brooks,Jr. "Force Display Performs Better than visual display in a simple 6-D docking task," *Proceedings of the IEEE International Conference on Robotics and Automation*, 1989, pp. 1462-66.

[13] M. G. Mohamed. *Instantaneous kinematics and joint displacement analysis of fully-parallel robotic devices*. Ph.D. thesis, Department of Mechanical Engineering, University of Florida, 1983.

[14] M. Russo. "Implementation of a three DOF, motor/brake hybrid force output device for virtual environment control tasks," Abstract from *Engineering Foundation Conference on Man-Machine Interfaces for Teleoperation and Virtual Environments*, Santa Barbara, CA, March, 1990.